NANO LETTERS

Letter

pubs.acs.org/NanoLett

Conformal and Atomic Characterization of Ultrathin CdSe Platelets with a Helical Shape

Eline M. Hutter,[†] Eva Bladt,[‡] Bart Goris,[‡] Francesca Pietra,[§] Johanna C. van der Bok,[†] Mark P. Boneschanscher,[†] Celso de Mello Donegá,[†] Sara Bals,[‡] and Daniël Vanmaekelbergh*[,†]

[†]Condensed Matter and Interfaces, Debye Institute for Nanomaterials Science, Utrecht University, Princetonplein 1, 3584 CC Utrecht, The Netherlands

[‡]Electron Microscopy for Materials Research (EMAT), University of Antwerp, Groenenborgerlaan 171, 2020 Antwerp, Belgium

[§]Opto-electronic Materials Section, Department of Chemical Engineering, Delft University of Technology, Julianalaan 136, 2628 BL Delft, The Netherlands

S *Supporting Information*

ABSTRACT: Currently, ultrathin colloidal CdSe semiconductor nanoplatelets (NPLs) with a uniform thickness that is controllable up to the atomic scale can be prepared. The optical properties of these 2D semiconductor systems are the subject of extensive research. Here, we reveal their natural morphology and atomic arrangement. Using cryo-TEM (cryo-transmission electron microscopy), we show that the shape of rectangular NPLs in solution resembles a helix. Fast incorporation of these NPLs in silica preserves and immobilizes their helical shape, which allowed us to perform an in-depth study by high angle annular dark field scanning transmission electron microscopy (HAADF-STEM). Electron tomography measurements confirm and detail the helical shape of these systems. Additionally, high-resolution HAADF-STEM shows the thickness of the NPLs on the atomic scale and furthermore that these are consistently folded along a ⟨110⟩ direction. The presence of a silica shell on both the top and bottom surfaces shows that Cd atoms must be accessible for silica precursor (and ligand) molecules on both sides.

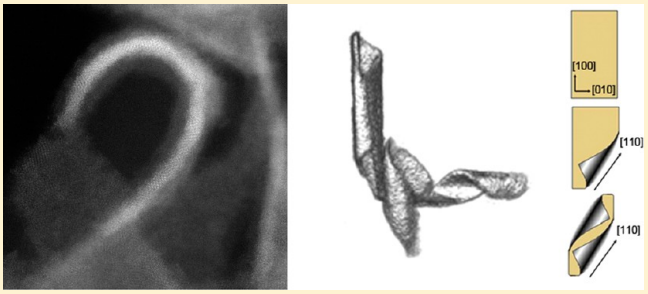

KEYWORDS: *2D semiconductor nanocrystals, CdSe nanoplatelets, nanohelices, silica coating*

Recent developments in colloidal synthesis have enabled the synthesis of 2D colloidal semiconductor nanocrystals with well-defined atomic thickness.[1−6] In the case of CdSe, these so-called nanoplatelets (NPLs) are often zinc blende crystals of only a few CdSe units thick with lateral dimensions in the range of tens of nanometers. As the thickness of the NPLs is much smaller than the exciton Bohr radius, while the lateral dimensions are much larger, these systems can be considered as suspended semiconductor quantum wells, with strong one-dimensional quantum confinement.[7] CdSe NPLs show a remarkably strong luminescence, and the first two exciton resonances are determined by their thickness.[7,8] At present, the optical transitions, which exhibit only homogeneous broadening, are extensively investigated.[5,9−13]

Ultrathin CdSe NPLs with lateral dimensions in the order of hundreds of nanometers are often observed as rolled-up scrolls of a few nanometers in diameter.[1,6,14−16] In contrast, when CdSe NPLs with the same thickness but much smaller lateral dimensions (i.e., tens of nanometers) are studied by electron microscopy, these are typically strongly wrinkled.[3,14,17] However, it remains unclear whether this wrinkled conformation is a natural state of these ultrathin NPLs (when suspended in the organic solution) or if it is due to drying effects or interaction with the substrate on the transmission electron microscopy (TEM) support grid. Although these ultrathin CdSe NPLs are expected to be very flexible, their conformal state in solution has not yet been precisely determined.

Here, we report a conformal study of ultrathin NPLs by cryo-TEM: the rapid freezing of a colloidal suspension should reveal the natural morphology of the suspended NPLs. We demonstrate that, for rectangular NPLs, this is close to helical. Furthermore, we incorporate CdSe NPLs emitting at 465 and 522 nm in a thin amorphous silica shell inside a reverse water-in-oil (w/o) microemulsion.[18−21] This method is based on a ligand exchange between the hydrophobic capping molecules on the surface of the NPLs and the silica precursor tetraethoxysilane (TEOS), prior to silica growth.[20,22] Following our previous work, we vary the concentration of the catalytically active ammonia to coat these ultrathin 2D anisotropic semiconductor nanocrystals with a well-defined silica shell.[23] At higher ammonia concentrations, it appears that the natural helical shape of the rectangular NPLs is preserved. We find that,

Received: July 8, 2014
Revised: October 20, 2014
Published: October 27, 2014

   dx.doi.org/10.1021/nl5025744 | *Nano Lett.* 2014, 14, 6257−6262

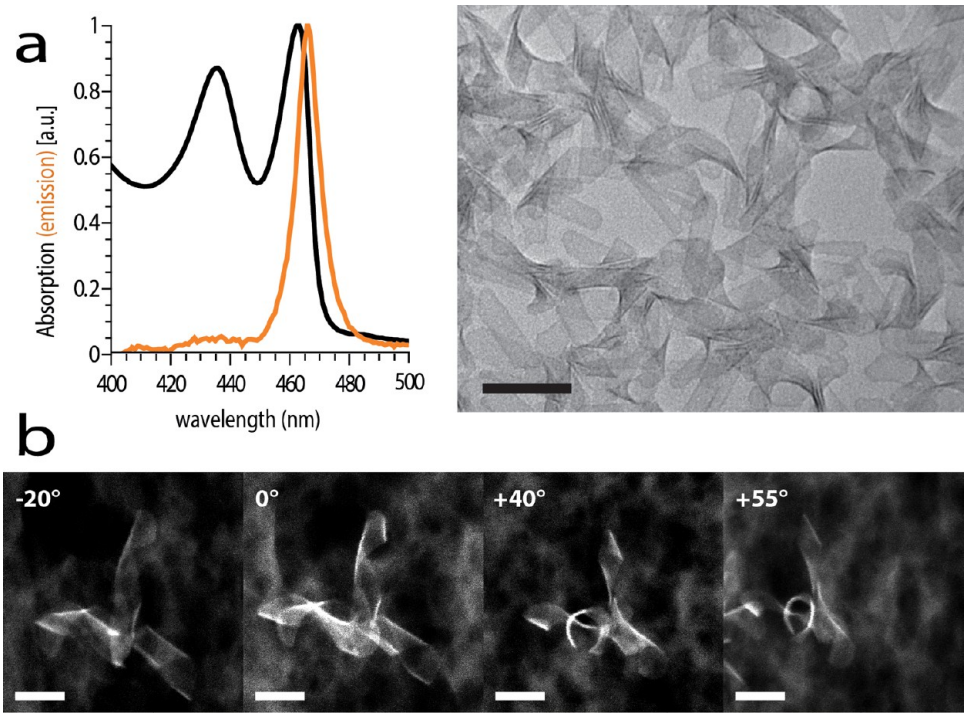

Figure 1. Ultrathin CdSe NPLs. (a) Absorption (black) and emission (orange) spectra and corresponding TEM image of ultrathin CdSe NPLs. The scale bar corresponds to 100 nm. (b) Cryo-TEM images of a group of CdSe NPLs in cyclohexane, viewed from different angles by tilting the TEM grid with respect to the detector. Scale bars correspond to 50 nm.

if the silica shell is grown sufficiently slow (i.e., at low ammonia concentrations), the CdSe NPLs have a rather flat conformation after encapsulation in silica, which has also been observed by coating with a CdS shell.[17] In both cases, we observe a comparable thickness of the silica layer on the top and bottom surfaces of the NPL.

Given that the rigid silica shell acts as a mechanical barrier against morphological changes, we are able to perform an in-depth study of the conformation and the atomic structure of the embedded NPLs with high-resolution high angle annular dark field scanning transmission electron microscopy (HAADF-STEM). Electron tomography at room temperature is used to determine the precise three-dimensional helical shape of the NPLs. High-resolution HAADF-STEM reveals that the helical NPLs emitting at 465 nm are only four CdSe monolayers (two unit cells) in thickness, whereas the NPLs emitting at 522 nm are five monolayers thick. The stoichiometric ratio between Cd and Se is confirmed by EDX measurements on a group of NPLs.

Considering that the initial growth is based on surface attachment of the negatively charged silica precursor,[22] the growth of a silica shell on both sides indicates that Cd atoms should be accessible for the silica precursor both on the top and the bottom surface. In this respect, a rearrangement of the atoms on the Se-terminated surface is required.[15] We believe that the change in surface energy resulting from this surface rearrangement is the cause of the observed helix conformation.

Figure 1a shows a TEM image of the ligand-stabilized CdSe NPLs (prior to silica-coating) dried on a TEM grid, together with absorption (black) and emission (orange) spectra. These sharp absorption and emission peaks are identical to those presented in the literature.[7] According to TEM, the lateral dimensions are 28 ± 7 nm by 80−140 nm. Furthermore, the TEM images of our NPLs suggest a strongly wrinkled state of the ultrathin sheets. However, these do not necessarily reflect the natural state of these systems in suspension, because drying effects and interaction with the grid may affect the morphology of these flexible NPLs. Cryo-TEM analysis of a frozen suspension is better suited to show the natural state of the NPLs and reveals that these rectangular NPLs are clearly helical (Figure 1b). Furthermore, the cryo-TEM images suggest that multiple NPLs are interconnected or at least attached to each other. The three-dimensional conformation of the NPLs is studied in more detail with electron tomography at room temperature (see below).

The CdSe NPLs emitting at 465 nm were incorporated in an amorphous silica shell with the reverse w/o microemulsion method,[18−22,24] which immobilizes their conformation. The HAADF-STEM images in Figure 2a show that the helical shape is perfectly preserved if the NPLs are coated with silica inside a microemulsion with 29.9 wt % ammonia in the aqueous phase. Morphologies other than helical-shaped are also observed; see top left image in Figure 2a. Following our recently developed method,[23] we also used relatively mild conditions (3.0 wt % ammonia, 3 h of growth) to coat the helical NPLs with an ultrathin uniform silica shell. This results in silica-coated helical-shaped CdSe NPLs that are no longer flexible (see Figure 2b). Figure 2c confirms that both the inner and the outer facet of the NPLs are covered with a silica shell that is between one and two nanometers thick. Interestingly, if we slow down the incorporation process even more (1.5 wt % ammonia), the NPLs are flattened after encapsulation in silica (Figure 2b). This rather flat conformation observed after slow growth of a silica shell is comparable to observations made when covering such CdSe NPLs with a CdS shell.[14,17] This unrolling has been attributed to a complete ligand exchange prior to the CdS shell growth,[17] which is also the case with 1.5 wt % ammonia: a complete ligand exchange occurs prior to silica nucleation along

dx.doi.org/10.1021/nl5025744 | Nano Lett. 2014, 14, 6257−6262

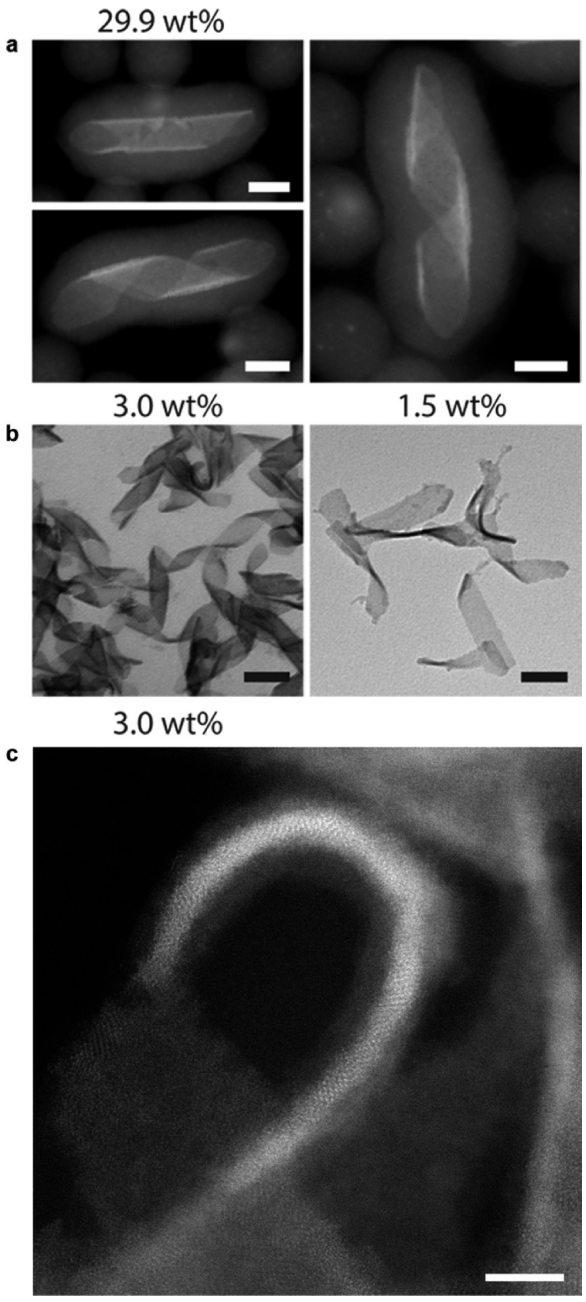

Figure 2. Images of CdSe NPLs coated with silica shells of different thickness. (a) HAADF-STEM images of silica-coated CdSe NPLs, quenched after 1 day of silica growth in a microemulsion to which 29.9 wt % ammonia was added. Scale bars correspond to 25 nm. (b) TEM images of CdSe NPLs coated with silica in a microemulsion with 3.0 wt % (left) and 1.5 wt % (right) ammonia, quenched after 3 h of growth. Scale bars correspond to 50 nm. (c) Top view of a folded NPL, taken from the sample presented in b (3.0 wt %), indicating the presence of silica at the top and bottom surface. The silica shell has a similar thickness on both sides (~2 nm). Scale bar corresponds to 5 nm.

the entire NPLs.[23] This yields uniformly silica-coated, nearly flat NPLs. In contrast, a high ammonia concentration leads to fast silica growth at the crystallographic facets at which the Cd atoms are the best accessible for the silica precursor molecules,[20,22,23,25] resulting in silica-coated helices. In general, the growth of a silica shell is not expected on a facet that is completely Se-terminated, since the negatively charged silica-precursor TEOS preferentially attaches to Cd.[25] Therefore, the observation that both the inside and the outside of the helical NPLs are covered with silica indicates the accessibility of Cd on both these facets.

The immobilization of the helical-shaped NPLs enabled us to perform an in-depth study of their conformation with HAADF-STEM tomography to further elucidate their geometry (see SI for movie). Figure 3 shows tomographic reconstructions of helical silica-coated NPLs. Similar to the cryo-TEM analysis of the NPLs prior to silica encapsulation (Figure 1), multiple helices are attached to each other with angles of 90°. Furthermore, the three-dimensional tomographic reconstructions confirm that the observed helices are indeed the 2D NPLs fully rotated over a diameter of ~25 nm, and hence most of the helices only make 1−1.5 twists. We should remark here that our helices are much shorter than any other reported helix of an inorganic material.[26−28] Furthermore, the helices are not preferentially left- or right-handed. Some of the NPLs fold into an "envelope" conformation, which is visible for the NPL along the *z*-direction in Figure 3 as well as the one shown in the top left image of Figure 2a.

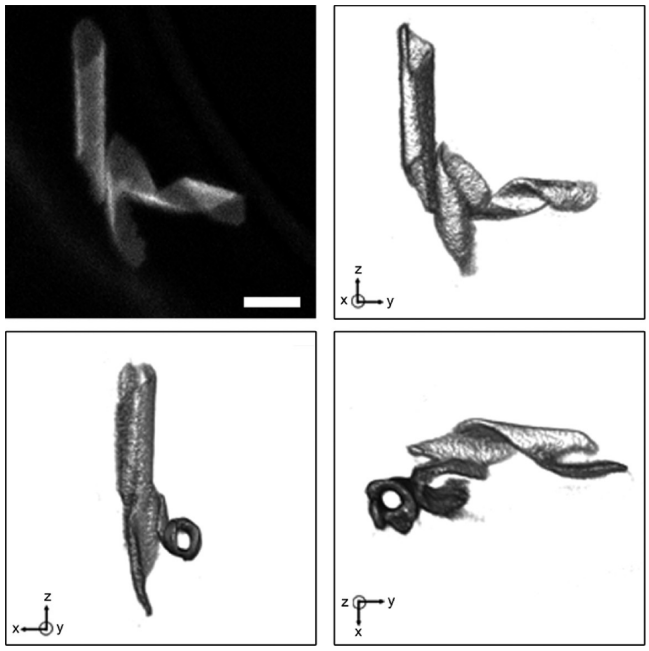

Figure 3. HAADF-STEM image and its 3D tomographic renderings at different viewing angles of silica-coated CdSe helices (3.0 wt % ammonia, 3 h of growth). An angle of 90° is present between two connected helical structures, similar to the observations from cryo-TEM shown in Figure 1b. Both left- and right-handed helices are observed. The scale bar corresponds to 20 nm.

Additionally, individual helical silica-coated NPLs (3.0 wt % ammonia) were studied with high-resolution HAADF-STEM, imaging the atomic structure of the helices from different directions. Figure 4 presents a high-resolution STEM projection showing the crystal lattice in the ⟨100⟩ viewing direction, which indicates that this NPL is folded along the ⟨110⟩ zone axis. Similar results obtained with other NPLs confirm that the platelets always fold along the ⟨110⟩ direction. Considering the helical and envelope-rolled morphologies of the silica-coated NPLs (Figure 3), together with the projection images, we can propose the following model of folding as

dx.doi.org/10.1021/nl5025744 | *Nano Lett.* 2014, 14, 6257−6262

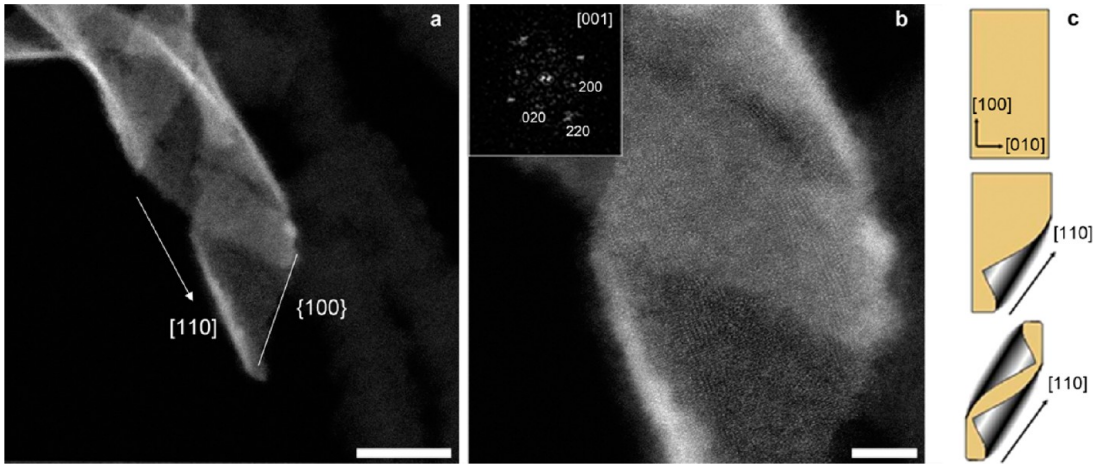

Figure 4. High-resolution HAADF-STEM images of silica-coated CdSe NPLs (3.0 wt % ammonia). (a–b) HAADF-STEM projection showing that the NPL folds along the ⟨110⟩ direction and that the large end-facets of the helical structures are {100} facets. Scale bars correspond to 20 and 5 nm, respectively. Inset: FT of the lower part. (c) Model showing the folding of the NPLs, starting from a rectangular sheet, the folding occurs along a ⟨110⟩ zone axis as visible in a–b.

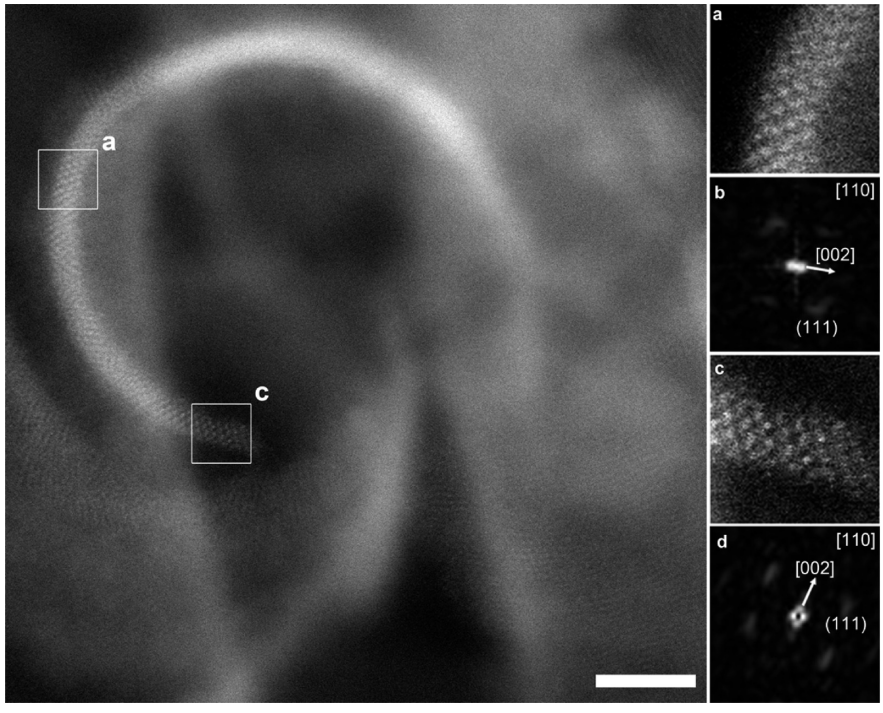

Figure 5. High-resolution HAADF-STEM image acquired along the ⟨110⟩ direction. (a, c) Detailed images showing that the NPLs consist of four CdSe units in their short direction (the white dots show the stronger scattering Cd atoms). Scale bar corresponds to 5 nm. (b,d) Fourier transforms of the highlighted regions (a,c) confirming that the NPLs fold along the ⟨110⟩ direction. The vector from the curved structure toward the center always points in a ⟨002⟩ direction.

presented in Figure 4c. This displays a flat rectangular NPL that curls along the [110] zone axis. Given that this axis forms a 45° angle with the [100] and [010] axes, the NPL now folds into (i) a helix if the [010] is short compared to the [100] and vice versa or (ii) an envelope-like structure (Figure S1) if the lateral dimensions are closer in length, i.e., if the NPL shape becomes closer to a square. Given that most of our CdSe NPLs were rectangular rather than square-shaped, their natural conformation in solution is closer to a helix. Often, two helices that are attached to each other are mutually orthogonal, which is clearly visualized by the tomographic reconstructions shown in Figure 3. This indicates the [110] growth direction of the cubic zinc blende structure.

In order to determine the thickness and curvature of the NPLs, high-resolution STEM projections of the silica-coated NPLs were acquired along the major axis of the helical structures; see Figure 5. The diameter of this curled structure is approximately 20 nm. The projection along the major axis again confirms the folding along a ⟨110⟩ direction, which is further proven by the fact that the vector from the edge of the structure toward the center of the curvature always corresponds to a [002] direction (see Figure 5b, d). The white dots represent the stronger scattering Cd atoms, and hence we observe a

dx.doi.org/10.1021/nl5025744 | *Nano Lett.* 2014, 14, 6257–6262

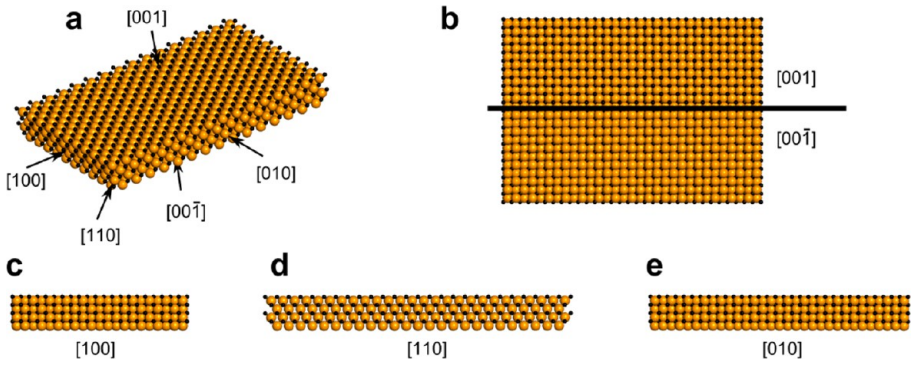

Figure 6. Crystallographic structure of a zinc blende CdSe NPL with a thickness of four monolayers, corresponding to two CdSe unit cells, with lateral dimensions of 10 × 15 unit cells (a). The larger Se atoms and smaller Cd atoms are represented by yellow and black spheres, respectively. In b, the top (Cd-terminated) and bottom (Se-terminated) surfaces are shown, corresponding to the inner and outer surface of the helices. Different side views of the NPL are shown in c–e. Note that the hexagonal arrangement of the Cd atoms in the [110] direction (d) is in agreement with the one observed in Figure 5 and Figure S3 (Supporting Information).

thickness of four monolayers of Cd as indicated in Figure 5a, c. Assuming that these NPLs are stoichiometric (as indicated by EDX measurements on a group of uncoated CdSe NPLs, see SI), this corresponds to a thickness of two CdSe unit cells. Considering these results, the pristine crystallographic structure of a CdSe NPL with a thickness of four monolayers (4 MLs) is now shown in Figure 6. If we take a closer look at the Cd atoms viewed from the top of the helix in Figure 5a and c, we find that they show a nonsymmetric hexagonal arrangement. This perfectly corresponds to the ⟨110⟩ direction of the zinc blende structure; see Figure 6d. Note that this is not the [111] direction, in which the Cd atoms are arranged in a symmetric hexagon.

Given that the observed folding of the CdSe NPLs after incorporation in silica represents their natural state in solution, our approach enables us to study the folding behavior of thicker NPLs as well. In contrast with the wrinkled state observed for 4 ML NPLs (Figure 1a), CdSe NPLs emitting at 522 nm usually appear flat when dried on a TEM support grid (see also Supporting Information, Figure S2).[1,14,17] Hence, to investigate their natural conformation, we incorporated CdSe NPLs with a lateral extension of 10–15 nm in a thin silica shell inside a reverse microemulsion (3.0 wt % ammonia, 3 h of growth) and studied these with HAADF-STEM (Supporting Information, Figure S3). Consistent with their emission at higher wavelength, HAADF-STEM shows that these NPLs consist of five rows of Cd in their short dimension, and hence we can conclude that the NPLs emitting at 522 nm are 5 MLs thick (i.e., 2.5 unit cell). Furthermore, similar to the 4 ML NPLs treated above (Figures 1–5), the natural state of these CdSe NPLs in solution is clearly not flat. Fourier transforms confirm that also these thicker NPLs have the tendency to curl along the ⟨110⟩ direction, although their lateral dimensions do not enable full rotation.

As mentioned above, the fact that silica grows equally well on both sides of the NPLs means that the Cd atoms, which coordinate the negatively charged silica precursor molecules (i.e., hydrolyzed TEOS) and native ligand molecules,[17] should be available on both sides. This is difficult to rationalize on the basis of the pristine crystallography of a stoichiometric NPL of which the shortest dimension is in the ⟨001⟩ direction (see Figure 6). That is, at the "Se-side" the Cd atoms cannot be easily approached for coordination with the ligand. However, as shown by a DFT study on CdSe nanosheets, the atoms on the surface can be rearranged to enable binding of the ligand molecules to Cd.[15] We believe that for our NPLs, a surface reconstruction on the Se-terminated facet induces them to adapt a folded conformation in solution, thereby lowering their total energy.

After incorporation of the 4 and 5 ML thick CdSe NPLs in silica, their photoluminescence is completely quenched. Furthermore, their absorption spectra substantially change, shifting to lower energies by tens of nanometers (hundreds of meV); see Figure 7 and Supporting Information, Figure S4. We measured comparable shifts in the absorption spectrum when coating CdSe/CdS core/shell NPLs with a silica shell (see Supporting Information, Figure S5). Although red-shifts in the absorption spectra after silica coating have been observed before for gold and semiconductor NCs, these are typically in the order of a few nanometers (i.e., a few tens of meV).[22,25,29−32] For these silica-coated 2D NPLs, the red-shifts are substantially larger, and hence it is unlikely that they originate solely from local field effects induced by the silica shell. In our opinion, the red shift is also due to leakage of the exciton wave function into the oxide monolayer that is bound to the surface Cd atoms, leading to a reduction of the strong 1D quantum confinement experienced by the exciton in the NPLs.

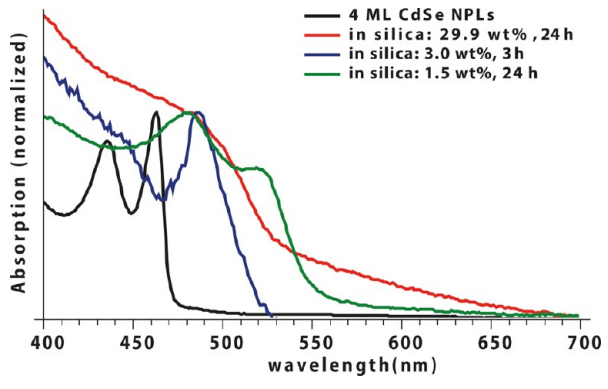

Figure 7. Absorption intensity (a.u.) for CdSe NPLs (black, corresponding to spectrum from Figure 1a), coated with silica in a microemulsion with 1.5 wt % ammonia (green line: 24 h) and 29.9 wt % ammonia (red line, 24 h) in the aqueous phase. The samples correspond to the silica-coated NPLs shown in Figure 2.

dx.doi.org/10.1021/nl5025744 | *Nano Lett.* 2014, 14, 6257–6262

In summary, we have revealed the natural morphology of ultrathin colloidal CdSe NPLs. With cryo-TEM we found that rectangular NPLs emitting at 465 nm have a *helical* shape in suspension. The thicker ones, emitting at 522 nm, show the propensity to fold in a similar way. The equal silica growth that we observed on the top and bottom surface shows that Cd atoms must be accessible for precursor molecules on both these surfaces. Furthermore, we were able to immobilize the helical NPLs by fast incorporation into a silica shell, which allowed us to study their conformation and atomic structure with HAADF-STEM microscopy and tomography. This analysis shows that the platelets are zinc blende, that the three main crystallographic axes belong to the ⟨100⟩ family, and that the helices are folded uniquely around the ⟨110⟩ axis. For the helices oriented with the ⟨110⟩ axis parallel to the beam, we could show that the NPLs emitting at 465 and 522 nm are 4 and 5 MLs CdSe in thickness, respectively.

We believe that our findings are of large importance for the future processing of suspensions of 2D semiconductors into material systems and for further understanding of their optical properties related to the atomic and conformal structure.

■ ASSOCIATED CONTENT

Ⓢ Supporting Information

One pdf containing experimental details concerning the synthesis of the CdSe NPLs and the coating with silica, details concerning the electron microcopy and tomography, and additional absorption spectra. One movie showing the reconstruction from Figure 3 in 3D. This material is available free of charge via the Internet at http://pubs.acs.org.

■ AUTHOR INFORMATION

Corresponding Author

*E-mail: d.vanmaekelbergh@uu.nl.

Author Contributions

E.M.H. and E.B. have contributed equally to this work.

Notes

The authors declare no competing financial interest.

■ ACKNOWLEDGMENTS

Dariusz Mitoraj, Hans Meeldijk, Relinde van Dijk-Moes, and Stephan Zevenhuizen are acknowledged for technical support and help with some experiments. The research leading to these results has received funding from the European Research Council under the European Union's Seventh Framework Programme (FP/2007-2013)/ERC Grant Agreement no. 291667. The authors acknowledge financial support from FOM and NOW [FOM program Functional NanoParticle Solids (FNPS)]. S.B. acknowledges financial support from European Research Council (ERC Starting Grant #335078-COLOURATOMS). E.B. and B.G. gratefully acknowledge financial support by the Flemish Fund for Scientific Research (FWO Vlaanderen).

■ REFERENCES

(1) Ithurria, S.; Dubertret, B. *J. Am. Chem. Soc.* **2008**, *130*, 16504−16505.

(2) Bouet, C.; Tessier, M. D.; Ithurria, S.; Mahler, B.; Nadal, B.; Dubertret, B. *Chem. Mater.* **2013**, *25*, 1262−1271.

(3) Ithurria, S.; Bousquet, G.; Dubertret, B. *J. Am. Chem. Soc.* **2011**, *133*, 3070−3077.

(4) Chen, Z.; Nadal, B.; Mahler, B.; Aubin, H.; Dubertret, B. *Adv. Funct. Mater.* **2014**, *24*, 295−302.

(5) Tessier, M. D.; Javaux, C.; Maksimovic, I.; Loriette, V.; Dubertret, B. *ACS Nano* **2012**, *6*, 6751−6758.

(6) Son, J. S.; Yu, J. H.; Kwon, S. G.; Lee, J.; Joo, J.; Hyeon, T. *Adv. Mater.* **2011**, *23*, 3214−3219.

(7) Ithurria, S.; Tessier, M. D.; Mahler, B.; Lobo, R. P. S. M.; Dubertret, B.; Efros, A. L. *Nat. Mater.* **2011**, *10*, 936−941.

(8) She, C.; Fedin, I.; Dolzhnikov, D. S.; Demortière, A.; Schaller, R. D.; Pelton, M.; Talapin, D. V. *Nano Lett.* **2014**, *14*, 2772−2777.

(9) Sigle, D. O.; Hugall, J. T.; Ithurria, S.; Dubertret, B.; Baumberg, J. J. *Phys. Rev. Lett.* **2014**, *113*, 087402.

(10) Tessier, M. D.; Biadala, L.; Bouet, C.; Ithurria, S.; Abecassis, B.; Dubertret, B. *ACS Nano* **2013**, *7*, 3332−3340.

(11) Biadala, L.; Liu, F.; Tessier, M. D.; Yakovlev, D. R.; Dubertret, B.; Bayer, M. *Nano Lett.* **2014**, *14*, 1134−1139.

(12) Kunneman, L. T.; Tessier, M. D.; Heuclin, H.; Dubertret, B.; Aulin, Y. V.; Grozema, F. C.; Schins, J. M.; Siebbeles, L. D. A. *J. Phys. Chem. Lett.* **2013**, *4*, 3574−3578.

(13) Achtstein, A. W.; Prudnikau, A. V.; Ermolenko, M. V.; Gurinovich, L. I.; Gaponenko, S. V.; Woggon, U.; Baranov, A. V.; Leonov, M. Y.; Rukhlenko, I. D.; Fedorov, A. V.; Artemyev, M. V. *ACS Nano* **2014**, *8*, 7678−7686.

(14) Bouet, C.; Mahler, B.; Nadal, B.; Abecassis, B.; Tessier, M. D.; Ithurria, S.; Xu, X.; Dubertret, B. *Chem. Mater.* **2013**, *25*, 639−645.

(15) Son, J. S.; Wen, X.-D.; Joo, J.; Chae, J.; Baek, S.-I.; Park, K.; Kim, J. H.; An, K.; Yu, J. H.; Kwon, S. G.; Choi, S.-H.; Wang, Z.; Kim, Y.-W.; Kuk, Y.; Hoffmann, R.; Hyeon, T. *Angew. Chem.* **2009**, *48*, 6861−6864.

(16) Li, Z.; Peng, X. *J. Am. Chem. Soc.* **2011**, *133*, 6578−6586.

(17) Mahler, B.; Nadal, B.; Bouet, C.; Patriarche, G.; Dubertret, B. *J. Am. Chem. Soc.* **2012**, *134*, 18591−18598.

(18) Selvan, S. T.; Tan, T. T.; Ying, J. Y. *Adv. Mater.* **2005**, *17*, 1620−1625.

(19) López-Quintela, M. . A. A. *Curr. Opin. Colloid Interface Sci.* **2003**, *8*, 137−144.

(20) Darbandi, M.; Thomann, R.; Nann, T. *Chem. Mater.* **2005**, *17*, 5720−5725.

(21) Arriagada, F. J.; Osseo-Asare, K. *Colloids Surf., A: Physicochem. Eng. Asp.* **1999**, *154*, 311−326.

(22) Koole, R.; van Schooneveld, M. M.; Hilhorst, J.; Donegá, C.; de, M.; 't Hart, D. C.; van Blaaderen, A.; Vanmaekelbergh, D.; Meijerink, A. *Chem. Mater.* **2008**, *20*, 2503−2512.

(23) Hutter, E. M.; Pietra, F.; van Dijk - Moes, R. J. A.; Mitoraj, D.; Meeldijk, J. D.; de Mello Donegá, C.; Vanmaekelbergh, D. *Chem. Mater.* **2014**, *26*, 1905−1911.

(24) Nann, T.; Mulvaney, P. *Angew. Chem., Int. Ed.* **2004**, *43*, 5393−5396.

(25) Pietra, F.; van Dijk - Moes, R. J. A.; Ke, X.; Bals, S.; van Tendeloo, G.; Donegá, C. D. M.; Vanmaekelbergh, D. *Chem. Mater.* **2013**, *25*, 3427−3434.

(26) Gao, P. X.; Ding, Y.; Mai, W.; Hughes, W. L.; Lao, C.; Wang, Z. L. *Science* **2005**, *309*, 1700−1704.

(27) Xie, J.; Qiu, H.; Che, S. *Chem.—Eur. J.* **2012**, *18*, 2559−2564.

(28) Jung, J. H.; Kobayashi, H.; van Bommel, K. J. C.; Shinkai, S.; Shimizu, T. *Chem. Mater.* **2002**, *14*, 1445−1447.

(29) Darbandi, M.; Lu, W.; Fang, J.; Nann, T. *Langmuir* **2006**, *22*, 4371−4375.

(30) Tan, T. T.; Selvan, S. T.; Zhao, L.; Gao, S.; Ying, J. Y. *Chem. Mater.* **2007**, *19*, 3112−3117.

(31) Hu, X.; Gao, X. *Phys. Chem. Chem. Phys.* **2012**, *13*, 10028−10035.

(32) Pastoriza-Santos, I.; Pérez-Juste, J.; Liz-Marzán, L. M. *Chem. Mater.* **2006**, *18*, 2465−2467.